The Dark Side of Hydrogen Bonds in the Design of Optical Materials: A Charge-Density Perspective

ARTICLE *in* CHEMISTRY - A EUROPEAN JOURNAL · MARCH 2014

Impact Factor: 5.73 · DOI: 10.1002/chem.201300566 · Source: PubMed

3 AUTHORS, INCLUDING:

Konstantin A Lyssenko
Russian Academy of Sciences
761 PUBLICATIONS **6,098** CITATIONS

ChemPubSoc Europe

DOI: 10.1002/chem.201300566

CHEMISTRY
A European Journal
Full Paper

Charge-Density Calculations

The Dark Side of Hydrogen Bonds in the Design of Optical Materials: A Charge-Density Perspective

Yulia V. Nelyubina,*[a] Lada N. Puntus,[b] and Konstantin A. Lyssenko[a]

Abstract: A combined investigation of the structural, electronic, and optical properties of three crystalline nonaaqualanthanoid(III) triflates, $[Ln(H_2O)_9(CF_3SO_3)_3]$, has provided unambiguous experimental evidence for charge redistribution in the first coordination sphere of a lanthanide ion as a result of hydrogen bonds with outer-sphere anions. As well as resulting in charge transfer from the noncoordinated anions to the coordinated water molecules, these hydrogen bonds give rise to a new excited state, an hydrogen-bond-induced charge-transfer state, which is observed experimentally for the first time. This state was shown to be responsible for the previously unknown negative aspect of hydrogen bonds with a lanthanide-bound water molecule: rather than increasing the luminescence efficiency of the complex, they can lead to additional quenching that is unfavorable for the task-specific design of optical materials.

Introduction

Lanthanide (Ln) complexes are of special interest as perspective emissive components for new optical materials.[1–5] In the case of Eu^{3+} and Tb^{3+} ions, the presence of water molecules in their first coordination sphere, an occurrence that is sometimes inevitable, results in a quenching of luminescence owing to multiphonon nonradiative relaxation by O–H oscillators.[6–8] This effect becomes more pronounced as a water molecule approaches the metal center. Recently, it was shown that involvement of metal-bound water molecules in hydrogen bonding with outer-sphere species can serve as a factor to reduce the quenching effect.[2,9] At the same time, systems are known[10–14] where the water molecule that forms stronger hydrogen bonds is the one with the shorter $Ln–OH_2$ distance, so an increase in the quenching of the luminescence would be formally expected. While the first, that is, positive aspect, of hydrogen bonding is now to be used for beneficial purposes in the design of optical materials, the second one (clearly unfavorable) has been observed neither theoretically nor experimentally.

To reveal if there is indeed a "negative side" of such hydrogen bonding with a metal-bound water molecule and, if so, what is the reason behind it, a series of crystalline nonaaqualanthanoid(III) triflates,[13,15] $[Ln(H_2O)_9(CF_3SO_3)_3]$—those of neodymium (**Nd1**), europium (**Eu1**) and terbium (**Tb1**)—was chosen (Figure 1) in which the metal ion is shielded by a hydrate shell and does not interact directly with the chelating ligands and/or counterions. Nevertheless, there is a distinct difference between the Ln–O bond lengths for each different coordinated water molecule within the complex, an observation that is clearly related to their different involvement in intermolecular contacts.[13,16–18]

The most informative approach to describe such an interplay between the Ln–O and hydrogen bonds on the quantitative level is the topological analysis of electron density distribution, $\rho(r)$,[19] in a crystal within Bader's quantum theory of "Atoms in Molecules" (QTAIM).[20] In addition to distinguishing bonding (stabilizing) interactions from all other contacts based on the bond critical points (3, −1) or BCP search, it allows for highly accurate estimation of their energies.[21–23] Good estimates have thus been obtained for various types of interactions, including those that involve heavy elements[24,25] such as lanthanide ions.[12]

To differentiate the role of hydrogen bonds in the lanthanide-to-water binding, we performed a high-resolution X-ray diffraction (XRD) investigation[26] of the complexes **1**, (Figure 1; see also Figures 1 and 3 in the Supporting Information) followed by QTAIM analysis of $\rho(r)$ functions, together with time-dependent-DFT (TD-DFT) calculations and luminescence studies of their single crystals.

Results and Discussion

In the crystals **1**, the metal cation (lying on a $\bar{6}$ axis) is surrounded by nine water molecules in such a manner that their oxygen atoms are located at the vertices of a tricapped trigonal prism.[13,15] The complex ion $Ln(H_2O)_9^{3+}$ (Ln = Nd, Eu, Tb) as a whole has $\bar{6}$ symmetry, with two independent positions of water molecule in the crystal, namely $H_2O(1W)$ and $H_2O(2W)$,

[a] Dr. Y. V. Nelyubina, Prof. K. A. Lyssenko
A.N. Nesmeyanov Institute of Organoelement Compounds
Russian Academy of Sciences
119991, Vavilova Str., 28, Moscow (Russia)
E-mail: unelya@xrlab.ineos.ac.ru

[b] Dr. L. N. Puntus
Institute of Radioengineering and Electronics, Russian Academy of Sciences
125009, Mokhovaya Str., 11-7, Moscow (Russia)

Supporting information for this article is available on the WWW under http://dx.doi.org/10.1002/chem.201300566.

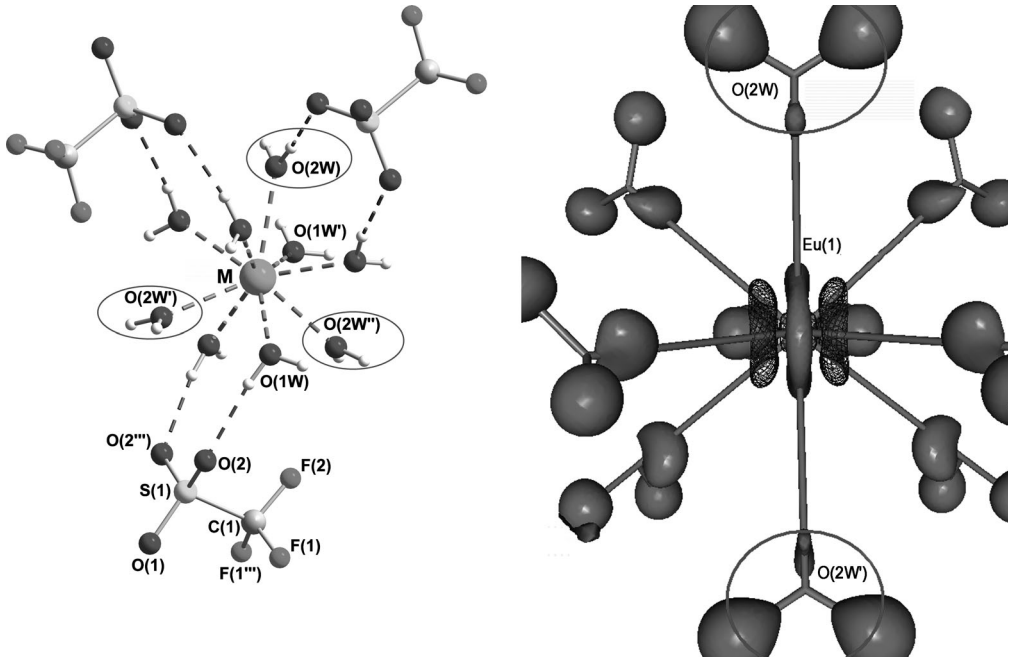

Figure 1. Left: General view of the complexes **1** (M = Nd, Eu, or Tb). Equatorial water molecules are highlighted by ovals. Right: Experimental 3D-distribution of the deformation electron density (DED) showing charge accumulation domains attributed to the lanthanide atom's 4f orbitals and oxygen atoms' lone pairs. Isosurface of DED equal to 0.3 e Å^{-3} is shown as solid; the negative one (−0.3 e Å^{-3}) is shown as a wireframe.

which occupy the axial and equatorial sites, respectively. As a result, the first coordination sphere of the lanthanide ion consists of three symmetry-related water molecules of type H_2O(2W) in the equatorial plane and six others of the H_2O(1W) type at the corners of the trigonal prism, all related by either a threefold-symmetry axis or an equatorial mirror plane (Figure 1).

The luminescence data for the complex with a europium(III) ion (as a useful luminescence probe) also indicate the relatively high symmetry of its coordination environment. Indeed, the luminescence spectrum of **Eu1** displays $^5D_0 \rightarrow {}^7F_J$ ($J = 0$–4) and $^5D_0 \rightarrow {}^7F_J$ ($J = 0$–2) transitions, with the magnetic dipole $^5D_0 \rightarrow {}^7F_1$ transition being the strongest. The ratio of the integrated intensity of the $^5D_0 \rightarrow {}^7F_2$ transition to that of the $^5D_0 \rightarrow {}^7F_1$ transition (a ratio that is generally accepted as a measure of asymmetry around a Eu^{3+} ion[27,28]) is < 1 (~0.4; Figure 2).

The distance from the metal center to the equatorial water molecule is markedly larger (2.5581(7) Å in **Nd1**, 2.5274(6) Å in **Eu1**, and 2.5163(5) Å in **Tb1**) than to the axial one (2.4643(5), 2.4210(4), and 2.3922(3) Å, respectively). This variation in the Ln–O bond lengths is in accordance with the differences in the interionic interactions linking the corresponding water molecules with the outer-sphere anions. Thus, the hydrogen bonds in these complexes, two per each H_2O moiety, are characterized by $O_{water}\cdots O_{triflate}$ separations being 2.7506(9)–190(9) Å for the axial and 2.9018(8)–127(5) Å for the equatorial water species (Table 1 and S1–S3 in the Supporting Information).

The difference between the two Ln–O bond types is clearly observed in their topological parameters (Tables S1–S3 in the Supporting Information), those at the BCPs, of the electron density distributions in the crystals **1**. The Ln–O(1W) bonds

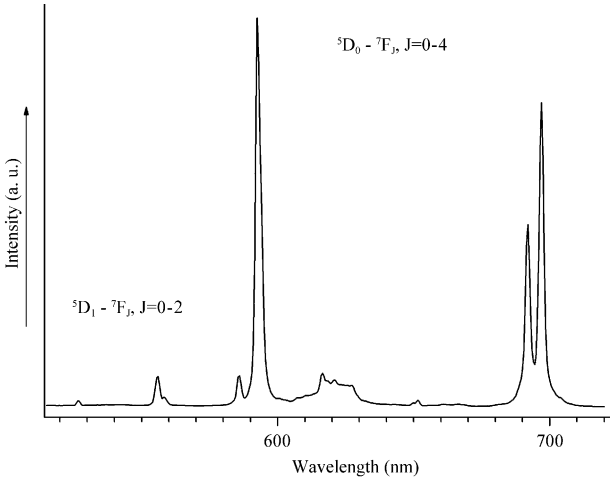

Figure 2. Luminescence spectrum of **Eu1** at 300 K ($\lambda_{exc} = 395$ nm).

Table 1. Differences in the Ln–O bond lengths Δ (Å) and energies dE (kcal mol^{-1}) with the complex **Tb1** as a "zero" point ($\Delta = R_{Ln\text{-}O}(Ln) - R_{Ln\text{-}O}(Tb)$, $dE = E_{int}(Ln) - E_{int}(Tb)$), and the corresponding values for hydrogen bonds in the crystals **1** according to the X-ray diffraction data.

	Ln = Nd	Ln = Eu		Ln = Nd	Ln = Eu
Δ[Ln–O(1W)]	0.073	0.029	*dE*[Ln–O(1W)]	−2.7	−1.0
Δ[Ln–O(2W)]	0.042	0.010	*dE*[Ln–O(2W)]	−0.4	1.0
Δ[O(1W)···O(1)]	0.000	0.000	*dE*[O(1W)···O(1)]	−0.3	−1.2
Δ[O(1W)···O(2)]	0.005	0.003	*dE*[O(1W)···O(2)]	0.6	0.5
Δ[O(2W)···O(2)]	−0.010	−0.005	*dE*[O(2W)···O(2)]	0.1	0.0

($\rho(r) = 0.31$–0.33 e Å^{-3}; $\nabla^2\rho(r) = 4.7$–5.6 e Å^{-5}; $h_e(r)$ varies from -0.0009 to -0.0002 a.u.) correspond to the intermediate interactions, whereas the Ln–O(2W) bonds are of the closed-shell type ($\rho(r) = 0.24$–0.27 e Å^{-3}; $\nabla^2\rho(r) = 3.9$–4.0 e Å^{-5}; $h_e(r) = 0.0006$–0.0023 a.u.). The $\rho(r)$ and $\nabla^2\rho(r)$ values in the BCPs of the hydrogen bonds are in the ranges of 0.09–0.21 e Å^{-3} and 1.6–2.8 e Å^{-5}, respectively, with a covalent contribution similar to that of the Ln–O bonds. Indeed, although interactions involving lanthanide ions are generally considered as fully ionic,[29,30] the negative electron energy densities, $h_e(r)$, for the Ln–O bonds provide evidence for their partially covalent character. The same follows from the luminescence data, namely from the experimental energy of the $^5D_0$ level of the Eu^{3+} ion (the nephelauxetic effect,[31] $E_{exp} = 17\,100$ cm^{-1}). Thus, a forbidden $^5D_0 \rightarrow {}^7F_0$ transition (region 575–580 nm) with a monoexponential luminescence decay ($\tau = 0.10 \pm 0.01$) is present as a symmetric line at ~585 nm/17 100 cm^{-1} at 300 K (Figure 2). Note that the obtained covalent contribution to the Ln–ligand bonding (the ligand being water molecules, among others) was previously found to exceed the corresponding one for chemical bonds formed by alkaline and alkaline earth metals.[12]

As estimated from the X-ray diffraction data on the basis of the Espinosa correlation,[32,33] that with the $v(r)$ value in the related BCP,[32] the energy (E_{int}) of the Ln–O bonds is 11.2–18.2 kcal mol^{-1} and correlates with the interatomic distance (see Figure S2 in the Supporting Information). Both of these values feature significant anisotropy owing to the lanthanide contraction.[34] Indeed, the corresponding variation in the Ln–O distances and energies for the axial water molecules is higher than those for the equatorial ones (Table 1). The shortening of the Ln–O(1W) bonds along the series by 0.073 Å is accompanied by a decrease in the interaction energy for the H_2O(1W) moiety by 2.7 kcal mol^{-1}. In the case of the equatorial water molecule, the largest difference is nearly half the size (0.042 Å and 1.0 kcal mol^{-1}).

Although the hydrogen bonds in the crystals **1**, ($E_{int} = 3.8$–7.4 kcal mol^{-1}) are weaker than the Ln–O ones, they are strong enough to distort the coordination sphere of the lanthanide ion (12.4–13.3 and 7.7–7.8 kcal mol^{-1} in total per axial and equatorial water molecule; see also Table 2). This agrees well with the equalization of the Ln–O bond lengths observed in isolated $Ln(H_2O)_9^{3+}$ cations.[35] This observation means that the two positions of water molecules are initially equivalent, hence indicating the incorrectness of the explanation proposed earlier for the elongation of the Ln–O bond with one water molecule as a result of it occupying a sterically demanding site.[17]

Table 2. Total energy of the Ln–O and hydrogen bonds (kcal mol^{-1}) as well as the net charge of the triflate anions (e) in the complexes **1**.

	Ln = Nd	Ln = Eu	Ln = Tb
Total Ln–O bond energy	126.5	140.3	143.6
Total hydrogen-bond energy	105.7	136.6	148.3
Net CF_3SO_3 charge	−0.16	−0.03	0.00

In the case of the complexes **1**, the hydrogen-bond energies vary by 1.2 kcal mol^{-1} for the axial water molecules and are practically the same (within 0.1 kcal mol^{-1}) for the equatorial ones, that is, the smaller the difference in the hydrogen-bond strength is, the smaller the change in the Ln–O distance is. Therefore, the lanthanide contraction depends on the type of water molecule bound to the lanthanide cation and, thus, is governed by the degree of "stiffness" of the hydrogen-bonded framework.[12]

Note that besides these hydrogen bonds, in the crystals **1**, there are only long O···O (3.2743(6)–572(5) Å) and F···F (2.9194(3)–852(6) Å) contacts between triflate anions, as well as contacts between F(anion)···O(water) (3.1334(6)–522(4) Å). All of these contacts display BCPs (Figure S3 in the Supporting Information), except for the longest F···F contact (3.0852(6) Å) in the neodymium complex. These interactions are very weak ($E_{int} = 0.6$–1.1 kcal mol^{-1}), which is a common feature of interactions between like-charged species,[36] and can have little effect on the Ln–O bonding.

To further relate the elongation of the Ln–O(2W) bonds with the peculiarities of supramolecular organization, we examined the distribution of charges in **1** (Table S4 in the Supporting Information). Although there is no reference data for the charge of lanthanide cations in a crystal owing to the fact that charge-density investigations of lanthanide salts are limited in number, the values obtained (+1.49, +1.45, and +1.41 e for Nd, Eu, and Tb, respectively) are quite reliable, being supported by very small "charge leakage" (not more than 0.01 e). Moreover, topological analysis of experimental electron density itself is more appropriate for the analysis of such compounds than theoretical methods. Indeed, both the calculated charge of a cation and the geometry for corresponding aqua complexes are extremely sensitive to method/basis set combinations as well as to the relativistic effective core potentials used.[35] Depending on the choice of the latter, the lanthanide charge can vary in a very broad range; in some cases its absolute value was found to even exceed the nominal charge of +3.

The net charges of other species clearly show that such a high difference between the estimated and formal charges of lanthanide cations is due to the coordinated water molecules effectively "pumping" the charge from the triflate anions through hydrogen bonding; the charge-transfer value being from 2.52 to 3.00 e (Table 2) per $Ln(H_2O)_9^{3+}$ moiety.

The resulting accumulation of charge on the water molecules is also confirmed by the following observations from the luminescence data. First, the above experimental energy of the $^5D_0$ level of the Eu^{3+} ion is quite far from the calculated one ($\Delta E_{calc-exp} = +180$ cm^{-1}); such a large difference is sugestive of additional charge accumulation on the coordinated water molecules. This follows from the well-known dependence of the nephelauxetic parameter on the charge of a coordinated atom: for comparison, the energy of the $^5D_0$ level of the Eu^{3+} ion in the aqua complex $[Eu(H_2O)_9]^{3+}$ with neutral water molecules is 17 280 cm^{-1} versus 17 232 cm^{-1} for $Eu(dipicolinate)_3^{3-}$ with carboxylate coordination sites.[37] The corresponding value for the complex **Eu1** is even lower, 17 100 cm^{-1}, which indi-

cates the higher negative charge of the oxygen atoms in the coordinated water molecules in comparison with both these cases; this clearly results from their hydrogen bonding with triflate anions.

Second, in the luminescence spectra of **Eu1** and **Tb1**, a structurally broad band, with vibronic progression $\approx 1225\ cm^{-1}$, attributed to a stretching vibration of the CF_3 group is observed in the region of 400–480 nm (Figures 2 and 3; see also Figure S4 in the Supporting Information). This observation indicates a vibronic interaction involving the Ln^{3+} ion and an uncoordinated triflate anion. An excited state is also observed in the excitation and absorption spectra of crystals **1** (310–330 nm; Figures S5 and S6 in the Supporting Information). It should be emphasized that owing to the similar energies of this excited state in the complexes **1**, with different lanthanide ions, it can be described as forming through charge transfer (CT) from an uncoordinated anion to a coordinated ligand (water molecules in this case) through the hydrogen bonds (hydrogen-bond-induced CT state, HbICT state).

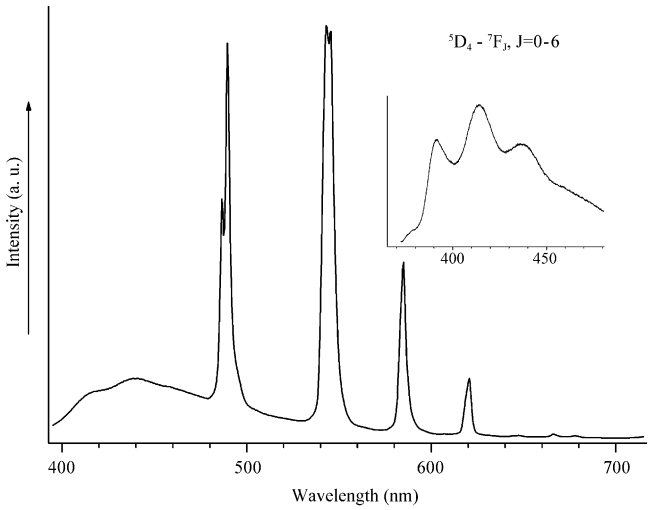

Figure 3. Luminescence spectrum of **Tb1** at 300 K ($\lambda_{exc} = 380$ nm). Insert: Part of the same spectrum measured at 77 K.

Finally, the nature of this HbICT state was proved by the TD-DFT calculations performed for a cluster containing the complex cation $Eu(H_2O)_9^{3+}$ surrounded by three triflate anions. The calculations showed the presence of the excited state (318 nm) corresponding to the transition from the HOMO, centered at the electron lone pairs of the oxygen atoms of the triflate groups, to the LUMO, centered at the water molecules hydrogen bonded with the corresponding triflate moieties (Figure 4), similar to those observed in the theoretical investigation of a series of aqua-based palladium triflates.[38] Although this previously unknown HbICT state would be a reason for the ineffective deactivation process, its other possible role is in expanding the excitation channels observed for Ln-containing complexes and also induced by supramolecular organization[10] should be taken into account.

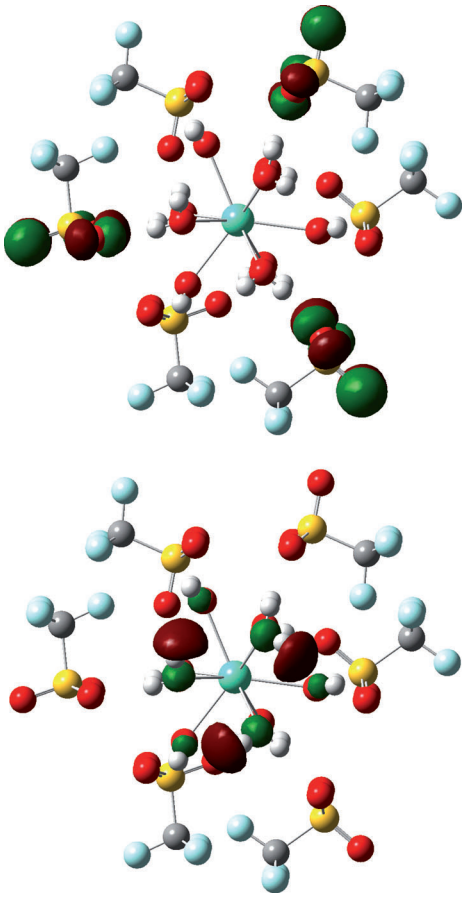

Figure 4. Schematic diagram of selected frontier orbitals illustrating the CT in **Eu1** (HOMO top and LUMO bottom).

The extents to which negative charge is concentrated on the independent water molecules in **1** are different; the net charge of the axial molecules is from −0.19 to −0.14 e and that for the equatorial ones from −0.10 to −0.06 e (the charge on their oxygen atoms varies from −1.17 to −1.09 e). This explains the cooperative relationship between the Ln–O and hydrogen bonds (Table 3). Indeed, the stronger hydrogen bonding of the axial water molecule ($\Sigma E_{H\text{-}bond}$ is 13.3 kcal mol^{-1} in **Nd1**, 12.4 kcal mol^{-1} in **Eu1**, and 13.1 kcal mol^{-1} in **Tb1**) leads to the greater accumulation of charge on it, which then causes it to bind more tightly to the lanthanide cation, and not vice versa. The energy of the corresponding Ln–O(1W) bond increases (15.5, 17.1, and 18.2 kcal mol^{-1} for neodymium, europium, and terbium complexes, respectively), and the interatomic

Table 3. Energy of the Ln-O and hydrogen bonds formed by axial and equatorial water molecules and net charges of the latter in the complexes **1**.

	$E_{Ln\text{-}O}$	$\Sigma E_{H\text{-}bond}$	H_2O charge
Nd–O(1W)/Nd–O(2W)	15.5/11.2	13.3/7.8	−0.14/−0.06
Eu–O(1W)/Eu–O(2W)	17.1/12.5	12.4/7.7	−0.17/−0.11
Tb–O(1W)/Tb–O(2W)	18.2/11.6	13.1/7.7	−0.19/−0.10

distance decreases. The hydrogen bonds formed by the equatorial water molecule are weaker ($\Sigma E_{H\text{-}bond}$ is 7.8 kcal mol^{-1} in **Nd1**, 7.7 kcal mol^{-1} in **Eu1**, and 7.7 kcal mol^{-1} in **Tb1**), and the corresponding charge transfer is less efficient, a fact that makes its binding with the lanthanide cation less favorable (11.2, 12.5, and 11.6 kcal mol^{-1} for neodymium, europium, and terbium complexes, respectively).

Conclusion

The combined investigation of structural, electronic, and optical properties of a series of lanthanide complexes, $[Ln(H_2O)_9(CF_3SO_3)_3]$, has provided unambiguous experimental evidence for charge redistribution within the first coordination sphere of a metal atom owing to hydrogen bonds with outer-sphere species. Resulting in a charge transfer from the noncoordinated anions to the coordinated water molecules, the hydrogen bonds govern the geometric parameters and electronic structure of these complexes as well as their optical properties. Thus, they give rise to an additional exited state that we identified as the hydrogen-bond-induced charge-transfer state. With no interfering contribution from other ligands, which are not present in these complexes, this is the first experimental observation of such a previously unknown HbICT state. Given that the hydrogen bonds in the crystals $[Ln(H_2O)_9(CF_3SO_3)_3]$ are of an average strength, many other systems are expected to have HbICT states, some of which may have a more pronounced effect on the luminescence sensitization. Although hydrogen bonding can serve as a convenient route to self-assembly for the design of new optical materials, any hydrogen bonds with metal-bound water molecules—especially the strongest ones (those with anions)—would clearly lead to the unfavorable quenching of the luminescence of lanthanide-containing complexes.

Experimental Section and Computational Methods

Crystallographic data

Crystals **1** were obtained by recrystallization of lanthanide triflates from ethanol. All spectroscopic measurements were performed on the crystals used for the X-ray diffraction investigation.

$[Nd(H_2O)_9(CF_3SO_3)_3]$ (Nd1): Crystals of **Nd1** ($C_3H_{18}NdF_9O_{18}S_3$, M_r = 753.59) are hexagonal, space group $P6_3/m$, at 100 K: a = 13.8824(8), b = 13.8824(8), c = 7.3283(9) Å, V = 1223.10(18) Å^3, Z = 2 (Z' = 1/6), d_{calc} = 2.046 g cm^{-3}, $\mu(Mo_{K\alpha})$ = 25.17 cm^{-1}, $F(000)$ = 738.

$[Eu(H_2O)_9(CF_3SO_3)_3]$ (Eu1): Crystals of **Eu1** ($CSS_3H_{18}EuF_9O_{18}S_3$, M_r = 761.31) are hexagonal, space group $P6_3/m$, at 100 K: a = 13.8059(2), b = 13.8059(2), c = 7.32280(10) Å, V = 1208.75(3) Å^3, Z = 2 (Z' = 1/6), d_{calc} = 2.092 g cm^{-3}, $\mu(Mo_{K\alpha})$ = 29.93 cm^{-1}, $F(000)$ = 744.

$[Tb(H_2O)_9(CF_3SO_3)_3]$ (Tb1): Crystals of **Tb1** ($C_3H_{18}TbF_9O_{18}S_3$, M_r = 768.27) are hexagonal, space group $P6_3/m$, at 100 K: a = 13.7473(2), b = 13.7473(2), c = 7.3364(2) Å, V = 1200.74(4) Å^3, Z = 2 (Z' = 1/6), d_{calc} = 2.125 g cm^{-3}, $\mu(Mo_{K\alpha})$ = 33.46 cm^{-1}, $F(000)$ = 748.

Intensities of 98 283, 97 022, and 167 631 reflections were measured for **Nd1**, **Eu1** and **Tb1**, respectively, with a Bruker SMART APEX2 CCD diffractometer [$\lambda(Mo_{K\alpha})$ = 0.71072 Å, ω-scans, $2\theta < 100$–120°]; then 4457, 6320, and 5362 independent reflections [R_{int} = 0.0408–0.0593] were used in further refinement. All structures were solved by direct method and refined by the full-matrix least-squares technique against F^2 in the anisotropic-isotropic approximation. The refinement converged to $wR2$ = 0.0405, GOF = 1.001, and $R1$ = 0.0181 for **Nd1**; $wR2$ = 0.0447, GOF = 1.004, and $R1$ = 0.0212 for **Eu1**; and $wR2$ = 0.0304, GOF = 1.001, and $R1$ = 0.0117 for **Tb1**. All calculations were performed by using SHELXTL PLUS 5.0.[39]

Calculations and refinement

Multipole refinement of **Nd1**, **Eu1**, and **Tb1** was carried out within the Hansen–Coppens formalism[40] by using the XD program package[41] with the core and valence electron density derived from wave functions fitted to a relativistic Dirac–Fock solution.[42] Before the refinement, the O–H bond distances were normalized to the values obtained from the statistical analysis of Inorganic Crystal Structure Database (ICSD) for similar structures. The level of multipole expansion was hexadecapole for the metal atoms and octupole for all other non-hydrogen atoms. The dipole D_{10} was refined for all hydrogen atoms. The refinement was carried out against F and converged to R = 0.0151, Rw = 0.0130, and GOF = 0.888 for **Nd1**; to R = 0.0198, Rw = 0.0142, and GOF = 0.935 for **Eu1**; and to R = 0.0105, Rw = 0.0118, and GOF = 0.841 for **Tb1**. The total electron-density function was positive everywhere, and the maxima of the residual electron density located in the vicinity of the metal nuclei were not more than 0.40 e Å^{-3}, which is quite low for compounds containing such heavy elements. Analysis of topology of the $\rho(r)$ function was carried out by using the WinXPRO program package.[43]

Electronic excitation energies were calculated with the time-dependent density-functional theory (TD-DFT) by using the Gaussian09 program package.[44] The hybrid B3LYP functional,[45,46] large-core energy-adjusted RECPs for Eu developed in the Stuttgart and Dresden groups, together with the accompanying basis sets to describe the valence electron density, were used. Large-core energy-adjusted RECPs for lanthanides put 5s, 5p, 6d, and 6s shells in the valence space, whereas 4f electrons belonged to the core pseudopotentials. The corresponding valence basis sets associated with the pseudopotentials are (6s6p5d) contracted to [4s4p4d].[47] For other atoms, a 6-31G** basis set was employed.

Luminescence measurements

Luminescence measurements (spectra and lifetimes) were performed on a Fluorolog FL 3-22 spectrometer from Horiba–Jobin–Yvon–Spex at 300 K and 77 K. The lifetimes were measured on samples in quartz capillaries; they are averages of at least three independent measurements, which were achieved by monitoring the decay at the maxima of the emission spectra. The single or bi-exponential decays were analyzed with the Origin 7.0 program. Attenuated-total-reflectance IR spectra were obtained from powdered samples with a PerkinElmer Spectrum One FTIR spectrometer. UV/Vis spectra of crystals, **1**, were obtained by using a Carl Zeiss M-40 spectrophotometer.

Acknowledgements

This study was financially supported by the Russian Foundation for Basic Research (Projects 12-03-33107, 13-03-00772, and 13-03-01041).

Keywords: charge-density redistribution · lanthanides · luminescence quenching · topological analysis · X-ray diffraction

[1] J. Leonard, C. Nolan, F. Stomeo, T. Gunnlaugsson in *Photochemistry and Photophysics of Coordination Compounds: Lanthanides*, Springer, Berlin Heidelberg, **2007**, pp. 1 – 43.
[2] J.-C. G. Bunzli, S. V. Eliseeva, *Chem. Soc. Rev.* **2010**, *39*, 189 – 227.
[3] S. Laurent, L. Vander Elst, R. N. Muller, *Q. J. Nucl. Med. Mol. Im.* **2009**, *53*, 586 – 603.
[4] C. M. Spangler, M. Schäferling in *Luminescent Chemical and Physical Sensors Based on Lanthanide Complexes, Vol. 7* (Eds.: P. Hänninen, H. Härmä), Springer, Berlin, **2011**, pp. 235 – 262.
[5] M. Schaferling, *Angew. Chem.* **2012**, *124*, 3590 – 3614; *Angew. Chem. Int. Ed.* **2012**, *51*, 3532 – 3554.
[6] Y. Haas, G. Stein, *J. Phys. Chem.* **1971**, *75*, 3677.
[7] G. Stein, E. Wurzberg, *J. Chem. Phys.* **1975**, *62*, 208.
[8] D. Parker, J. A. G. Williams, *Dalton Trans.* **1996**, 3613 – 3628.
[9] P. Wang, J.-P. Ma, Y.-B. Dong, *Chem. Eur. J.* **2009**, *15*, 10432 – 10445.
[10] L. N. Puntus, K. A. Lyssenko, I. S. Pekareva, J. C. G. Bunzli, *J. Phys. Chem. B* **2009**, *113*, 9265 – 9277.
[11] G. Bombieri, N. Marchini, S. Ciattini, A. Mortillaro, S. Aime, *Inorg. Chim. Acta* **2006**, *359*, 3405 – 3411.
[12] L. N. Puntus, K. A. Lyssenko, M. Y. Antipin, J.-C. G. Bunzli, *Inorg. Chem.* **2008**, *47*, 11095 – 11107.
[13] A. Chatterjee, E. N. Maslen, K. J. Watson, *Acta Crystallogr. Sect. B* **1988**, *44*, 381 – 386.
[14] Z. Baranyai, E. Gianolio, K. Ramalingam, R. Swenson, R. Ranganathan, E. Brucher, S. Aime, *Contr. Med. Mol. Imag.* **2007**, *2*, 94 – 102.
[15] A. Chatterjee, E. N. Maslen, K. J. Watson, *Acta Crystallogr. Sect. B* **1988**, *44*, 386 – 395.
[16] C. Apostolidis, B. Schimmelpfennig, N. Magnani, P. Lindqvist-Reis, O. Walter, R. Sykora, A. Morgenstern, E. Colineau, R. Caciuffo, R. Klenze, R. G. Haire, J. Rebizant, F. Bruchertseifer, T. Fanghänel, *Angew. Chem. Int. Ed.* **2010**, *49*, 6487 – 6491.
[17] D. Parker, H. Puschmann, A. S. Batsanov, K. Senanayake, *Inorg. Chem.* **2003**, *42*, 8646 – 8651.
[18] A. L. Thompson, D. Parker, D. A. Fulton, J. A. K. Howard, S. U. Pandya, H. Puschmann, K. Senanayake, P. A. Stenson, A. Badari, M. Botta, S. Avedano, S. Aime, *Dalton Trans.* **2006**, 5605 – 5616.
[19] C. Gatti, C. F. Matta, *Modern Charge-Density Analysis*, Springer, Berlin, **2012**.
[20] R. F. W. Bader, *Atoms In molecules. A Quantum Theory*, Clarendon, Oxford, **1990**.
[21] B. Dittrich, T. Koritsanszky, A. Volkov, S. Mebs, P. Luger, *Angew. Chem.* **2007**, *119*, 2993 – 2996; *Angew. Chem. Int. Ed.* **2007**, *46*, 2935 – 2938.
[22] Y. V. Nelyubina, I. V. Glukhov, M. Y. Antipin, K. A. Lyssenko, *Chem. Commun.* **2010**, *46*, 3469 – 3471.
[23] Y. V. Nelyubina, K. A. Lyssenko, *Chem. Eur. J.* **2012**, *18*, 12633 – 12636.
[24] Y. V. Nelyubina, M. Y. Antipin, D. S. Dunin, V. Y. Kotov, K. A. Lyssenko, *Chem. Commun.* **2010**, *46*, 5325 – 5327.
[25] A. O. Borissova, A. A. Korlyukov, M. Y. Antipin, K. A. Lyssenko, *J. Phys. Chem. A* **2008**, *112*, 11519 – 11522.
[26] CCDC 784551 (**Nd1**), 784552 (**Eu1**), and 784553 (**Tb1**) contain the supplementary crystallographic data for this paper. These data can be obtained free of charge from The Cambridge Crystallographic Data Centre via www.ccdc.cam.ac.uk/data_request/cif.
[27] A. F. Kirby, D. Foster, F. S. Richardson, *Chem. Phys. Lett.* **1983**, *95*, 507.
[28] A. F. Kirby, F. S. Richardson, *J. Phys. Chem.* **1983**, *87*, 2544.
[29] R. G. Lawrence, C. J. Jones, R. A. Kresinski, *J. Chem. Soc. Dalton Trans.* **1996**, 501 – 507.
[30] L. Petit, L. Joubert, P. Maldivi, C. Adamo, *J. Am. Chem. Soc.* **2006**, *128*, 2190 – 2191.
[31] S. T. Frey, W. d. W. J. Horrocks, *Inorg. Chim. Acta* **1995**, *229*, 383 – 390.
[32] E. Espinosa, E. Molins, C. Lecomte, *Chem. Phys. Lett.* **1998**, *285*, 170 – 173.
[33] E. Espinosa, I. Alkorta, I. Rozas, J. Elguero, E. Molins, *Chem. Phys. Lett.* **2001**, *336*, 457 – 461.
[34] C. Clavaguera, J.-P. Dognon, P. Pyykko, *Chem. Phys. Lett.* **2006**, *429*, 8 – 12.
[35] A. E. Clark, *J. Chem. Theory Comput.* **2008**, *4*, 708 – 718.
[36] Y. V. Nelyubina, M. Y. Antipin, K. A. Lyssenko, *Russ. Chem. Rev.* **2010**, *79*, 167 – 187.
[37] S. Cotton, *Lanthanide and Actinide Chemistry*, Wiley, Chichester, **2006**.
[38] G.-J. Zhao, K. L. Han, P. J. Stang, *J. Chem. Theory Comput.* **2009**, *5*, 1955 – 1958.
[39] G. M. Sheldrick, *Acta Crystallogr. Sect. A* **2008**, *64*, 112 – 122.
[40] N. K. Hansen, P. Coppens, *Acta Crystallogr. Sect. A* **1978**, *34*, 909 – 921.
[41] A. Volkov, P. Macchi, L. J. Farrugia, C. Gatti, P. Mallinson, T. Richter, T. Koritsanszky in XD2006—a computer program for multipole refinement, topological analysis of charge densities, and evaluation of intermolecular energies from experimental or theoretical structure factors, **2006**.
[42] Z. W. Su, P. Coppens, *Acta Crystallogr. Sect. A* **1995**, *51*, 27 – 32.
[43] A. Stash, V. Tsirelson, *J. Appl. Crystallogr.* **2002**, *35*, 371 – 373.
[44] Gaussian 09 (Revision C.01), M. J. Frisch, G. W. Trucks, H. B. Schlegel, G. E. Scuseria, M. A. Robb, J. R. Cheeseman, G. Scalmani, V. Barone, B. Mennucci, G. A. Petersson, H. Nakatsuji, M. Caricato, X. Li, H. P. Hratchian, A. F. Izmaylov, J. Bloino, G. Zheng, J. L. Sonnenberg, M. Hada, M. Ehara, K. Toyota, R. Fukuda, J. Hasegawa, M. Ishida, T. Nakajima, Y. Honda, O. Kitao, H. Nakai, T. Vreven, J. A. Montgomery, J. E. Peralta, F. Ogliaro, M. Bearpark, J. J. Heyd, E. Brothers, K. N. Kudin, V. N. Staroverov, R. Kobayashi, J. Normand, K. Raghavachari, A. Rendell, J. C. Burant, S. S. Iyengar, J. Tomasi, M. Cossi, N. Rega, N. J. Millam, M. Klene, J. E. Knox, J. B. Cross, V. Bakken, C. Adamo, J. Jaramillo, R. Gomperts, R. E. Stratmann, O. Yazyev, A. J. Austin, R. Cammi, C. Pomelli, J. W. Ochterski, R. L. Martin, K. Morokuma, V. G. Zakrzewski, G. A. Voth, P. Salvador, J. J. Dannenberg, S. Dapprich, A. D. Daniels, O. Farkas, J. B. Foresman, J. V. Ortiz, J. Cioslowski, Gaussian, Inc., Pittsburgh, PA, **2009**.
[45] A. D. Becke, *J. Chem. Phys.* **1993**, *98*, 5648 – 5652.
[46] P. J. Stephens, F. J. Devlin, C. F. Chabalowski, M. J. Frisch, *J. Phys. Chem.* **1994**, *98*, 11623 – 11627.
[47] J. Yang, M. Dolg, *Theor. Chem. Acc.* **2005**, *113*, 212 – 224.

Received: February 13, 2013
Revised: December 13, 2013
Published online on ■■ ▮▮, 0000

FULL PAPER

Be aware of the dark side: Investigation of the structural, electronic and optical properties of three $[Ln(H_2O)_9(CF_3SO_3)_3]$ complexes gives unambiguous experimental evidence for a charge redistribution in the first coordination sphere of the lanthanide ion as a result of hydrogen bonds between coordinated water molecules and outer-sphere anions (see figure). Rather than increasing the luminescence efficiency, these Hydrogen bonds lead to additional quenching that is unfavorable for the task-specific design of optical materials.

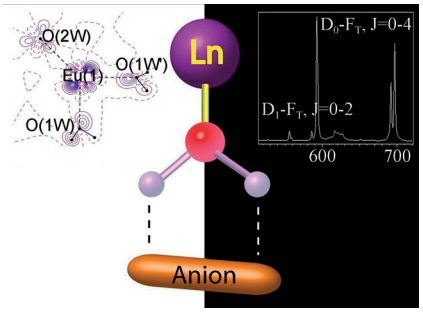

Charge-Density Calculations

Y. V. Nelyubina, L. N. Puntus, K. A. Lyssenko*

■■ – ■■

The Dark Side of Hydrogen Bonds in the Design of Optical Materials: A Charge-Density Perspective